Separation Science and Technology
Publication details, including instructions for authors and subscription information:
http://www.informaworld.com/smpp/title~content=t713708471

Mass Transfer Characteristics of Bale-Type Catalytic Distillation Packings

Efraín Manduca[a]; J. Castor González[b]; Hinda Elman[a]
[a] Chemical Engineering School, Universidad Central de Venezuela, Caracas, Venezuela [b] PDVSA-Intevep, Urb. Santa Rosa, Miranda, Venezuela

Online publication date: 08 November 2003

To cite this Article Manduca, Efraín , González, J. Castor and Elman, Hinda(2003) 'Mass Transfer Characteristics of Bale-Type Catalytic Distillation Packings', Separation Science and Technology, 38: 14, 3535 — 3552
To link to this Article: DOI: 10.1081/SS-120023415
URL: http://dx.doi.org/10.1081/SS-120023415

MARCEL DEKKER, INC. • 270 MADISON AVENUE • NEW YORK, NY 10016

SEPARATION SCIENCE AND TECHNOLOGY
Vol. 38, No. 14, pp. 3535–3552, 2003

Mass Transfer Characteristics of Bale-Type Catalytic Distillation Packings

Efraín Manduca,[1] J. Castor González,[2] and Hinda Elman[1,*]

[1]Universidad Central de Venezuela, Chemical Engineering School, Caracas, Venezuela
[2]PDVSA-Intevep, Urb. Santa Rosa, Los Teques, Miranda, Venezuela

ABSTRACT

The aim of this work was to evaluate the mass-transfer efficiency of the bale-type catalytic distillation packing as function of its main physical properties: external surface area and amount of catalyst. The overall gas phase mass-transfer coefficient and HETP values were calculated from experimental data. Experiments were carried out absorbing CO_2 in an aqueous solution of mono-ethanol-amine (MEA), using packings of different physical properties in a laboratory column of 1-in. diameter. The results show that the main mass transfer resistance is in the liquid phase and that the external area and amount of catalyst of the packing enhance the vapor–liquid mass-transfer rate. Several mass transfer models were evaluated but none of them properly reproduces the experimental data.

*Correspondence: Dr. Hinda Elman, Universidad Central de Venezuela, Chemical Engineering School, Caracas, Venezuela; E-mail: jhielman@cantv.net.

DOI: 10.1081/SS-120023415 0149-6395 (Print); 1520-5754 (Online)

INTRODUCTION

Catalytic distillation is a process that allows two simultaneous operations in a piece of single equipment: a chemical reaction and the separation of species by distillation. The main advantage of this technology is the application to reactions that are thermodynamically limited, when reactants and products have different relative volatilities. In this case, it is possible to significantly improve reaction yields with large savings in investment and operating costs.[1]

In the last decade, several processes have come to the market that use the catalytic distillation process. In this type of column, the packing contains a solid catalyst that promotes the chemical reaction. One of the most used catalytic packing is the so-called bale-type packing. However, very little has been published about the mass transfer behavior of this type of packing. This work shows a detailed evaluation of the mass transfer characteristics of the bale type packings, and the effect of properties such as surface area and amount of catalyst.

To perform this study, 1-in. diameter column was filled with bale packings and CO_2 was absorbed from air using an aqueous solution of mono-ethanol-amine (MEA). The overall mass-transfer coefficient and the height equivalent to a theoretical plate (HETP) were calculated from the experimental data.

There are various models to predict the mass-transfer coefficient of random and structured packings, based on different theories. Onda et al.[2,3] developed a model for random packing based on a modest set of data, using the double film theory. Bravo and Fair[4] used the Onda model with the large database of Bolles and Fair[5] to provide a correlation for the effective interfacial area, also for random packings.

A detailed knowledge of the hydraulic behavior is very important, not only for the design of the column, but also for the prediction of the mass-transfer efficiency[6] because there is a large dependence of the effective interfacial area with hydraulics. Hydraulic models for structured and random packings have been used for the simulation of catalytic distillation columns.[7–9]

Subawalla et al.[10] developed a model that predicts pressure drop, capacity, and HETP for catalytic distillation packings as function of parameters such as surface area and void fraction.

Aroonwilas et al.[11] studied the mass transfer behavior of structured packings for CO_2 absorbers with chemical reactions, employing aqueous solutions of NaOH, MEA, and AMP. They studied packing performance by examining the effect of operating parameters such as gas and liquid load, CO_2

partial pressure, liquid temperature, solvent concentration, and structured packing type on volumetric overall mass-transfer coefficient.

The results obtained by Aroonwilas et al. showed that the gas load does not have a significant effect on the mass-transfer coefficient and that the increase of the CO_2 partial pressure leads to a reduction of the rate of mass transfer due to diffusional effects. On the other hand, when the solvent concentration, temperature, or liquid load are increased, there was an improvement in the mass-transfer coefficient.

Caetano[12] used the air–water system, in conjunction with the same equipment used in this work (1-in. diameter column of 54-in. length) to evaluated the hydraulic behavior of bale-type catalytic packings. Caetano evaluated three sets of bale-type packings with different physical properties (catalyst content and specific surface). Caetano's results are of great importance for this work, since they provided all the hydraulic background required for the proper interpretation of this work.

ABSORPTION WITH CHEMICAL REACTION

In the physical absorption processes, the molar flux can be expressed in terms of the driving force using the mass-transfer coefficient:

$$N_A = k_L^0 \cdot (C_A - C_{Ai}) = k_G \cdot (P_A - P_{Ai}) \tag{1}$$

The k_L^0 mass-transfer coefficient is purely a physical coefficient. When there is a chemical reaction taking place in the liquid phase, the mass-transfer coefficient of the gas side is not affected, but the observed mass-transfer coefficient of the liquid side changes. The relation between the liquid side coefficients, with and without chemical reactions, is known as the enhancement factor and can be expressed as follows:

$$E = \frac{k_L}{k_L^0} \geq 1 \tag{2}$$

Where k_L is the enhanced liquid-phase mass-transfer coefficient, defined in terms of a concentration driving force.

As previously mentioned, in this work, a chemical system of CO_2–air (gas phase) and aqueous MEA (liquid phase) was used. The chemical reaction between MEA and CO_2 is a second-order exothermic reaction, where the mass transfer resistance is mainly in the liquid phase.[13]

$$CO_2 + 2RNH_2 \rightarrow RNHCOO^- + RNH_3{}^+ \tag{3}$$

For a second-order reaction, the variation of the solute concentration in the interphase film can be expressed as follows[14]:

$$D_{CO_2} \cdot \frac{d^2 C_{CO_2}}{dz^2} - k_2 \cdot C_{CO_2} \cdot C_{RNH_2} = 0 \tag{4}$$

The analytical solution of this equation is very complex, but it has been found that an accurate solution can be obtained using the enhancement factor.[14]

$$N_A = k_L^0 \cdot E \cdot (x_{Ai} - x_A) \tag{5}$$

The enhancement factor (E) of an irreversible second-order reaction can be calculated from the following equations.[14]

$$E = \frac{\sqrt{M \frac{E_i - E}{E_i - 1}}}{tan\, h \sqrt{M \frac{E_i - E}{E_i - 1}}} \tag{6}$$

$$M = \frac{D_L \cdot k_2 \cdot C_{STE}}{(k_L^0)^2} \tag{7}$$

$$E_i = \left(1 + \frac{D_{STE} \cdot C_{STE}}{z \cdot D_L \cdot C_{Ai}}\right) \tag{8}$$

The M parameter is a nondimensional constant obtained when Eq. (4) is solved and the E value corresponds to the enhancement factor of the instantaneous reaction. The square root of M is commonly known as the Hatta number.

BALE-TYPE PACKING CHARACTERISTICS

The bale-type packing contains the catalyst inside the 1 to 2-in. pockets of the fiber-glass cloth, which is wrapped in spiral with a stainless steel mesh wire. Figure 1 shows the schematics of the bale-type packings. The mesh wire provides both structural strength and open space for the gas and liquid flow. The commercial size of the bales are 8–14-in. diameter and about 20 inches in height.[15] The catalyst and cloth typically uses between 30 to 50% of the total free volume of the column.[16]

Both sides of fiber-glass cloth are wetted and represent the surface area available for mass transfer.[10] Packing geometry is affected by the amount of fiber-glass cloth used and by the mass of catalyst loaded. The amount of cloth

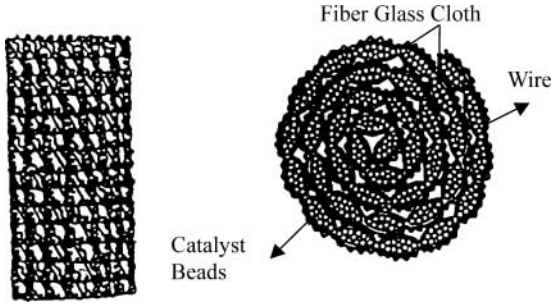

Figure 1. Sketches of bale-type catalytic packing.

used affects superficial area, and catalyst loading affects void fraction. Bales with higher catalyst densities (mass of catalyst per volume unit of column) have a lower void fraction and smaller channels available for two-phase flow.

MASS TRANSFER MODELS

The following models were used to predict the volumetric mass-transfer coefficients that were compared with experimental values.

Model of Subawalla et al.[10]: This model was developed to predict the pressure drop, capacity, and HETP of bale-type catalytic distillation packing. It was validated with data generated in a 2-in. diameter column distilling binary mixtures at total reflux. The model was developed assuming that the packing structure on the cloth surface of the bales makes a number of parallel channels with a dimension that can be calculated from the specific superficial area and the void fraction of the packing.

This model considers the mass transfer contribution of three main factors: the surface of the packing, the column walls, and the liquid drops. The following equation shows how these contributions are considered:

$$K_{OG}a_e = K_{OGp}a_{wetp} + K_{OGw}a_{wetw} + K_{OGg}a_g \tag{9}$$

The overall mass-transfer coefficients for each contribution are calculated from the individual phase coefficients using the double film theory as shown next:

$$\frac{1}{K_{OG}\cdot a_e} = \frac{1}{k_G\cdot a_e} + \frac{m}{k_L^0\cdot a_e} \tag{10}$$

The individual mass-transfer coefficients and effective area for each contribution are independently calculated for contribution.

Model of Bravo and Fair[4]: The model of Onda et al.[3] was modified by these investigators introducing an additional correlation to calculate the effective wetted area, as follows:

$$Ca_L = \frac{U_L \cdot \mu_L}{\sigma_L} \tag{11}$$

$$\frac{a_w}{a_p} = 1 - \exp\left(-0.45 \cdot \mathrm{Re}_L^{\,0.1} \cdot Fr_L^{\,-0.05} \cdot We_L^{\,0.2} \cdot \left(\frac{\sigma_c}{\sigma_L}\right)^{0.75}\right) \tag{12}$$

$$a_e = 0.489 \cdot a_p \cdot \sigma_L^{\,0.5} \cdot H^{-0.4} \cdot (Ca_L \cdot \mathrm{Re}_G)^{0.392} \tag{13}$$

The correlations to calculate the mass-transfer coefficients are the same originally proposed by Onda et al.

$$k_L = 0.0051 \cdot \left(\frac{\mu_L \cdot g}{\rho_L}\right)^{1/3} \cdot \left(\mathrm{Re}_L \cdot \frac{a_p}{a_w}\right)^{2/3} \cdot Sc_L^{\,-1/2} \cdot (a_e \cdot d_p)^{0.4} \tag{14}$$

$$k_G = 5.23 \cdot D_G \cdot a_p \mathrm{Re}_G^{\,0.7} \cdot Sc_G^{\,1/3} \cdot \left(a_p \cdot d_p\right)^{-2} \tag{15}$$

Model of Zheng and Xu[8,17]: This model was specifically developed for bale-type catalytic packings based on data from a 1.8-in. diameter columns. The equations to calculate the mass-transfer coefficients for each phase are expressed in terms of the Sherwood number as follows:

$$Sh_G = 0.072 \cdot 10^{-3} \cdot \mathrm{Re}_G^{\,0.92} \cdot Sc_G^{\,0.5} \tag{16}$$

$$Sh_L = 0.149 \cdot \mathrm{Re}_L^{\,0.30} \cdot Sc_L^{\,0.5} \tag{17}$$

Finally, it should be mentioned that all three models were developed from data for nonreactive systems. For this reason, it is necessary to introduce the chemical reaction enhancement factor in the calculation of the overall mass-transfer coefficient. This is achieved substituting Eq. (2) in Eq. (10) to give:

$$\frac{1}{K_{OG} \cdot a_e} = \frac{1}{k_G \cdot a_e} + \frac{m}{E \cdot k_L^0 \cdot a_e} \tag{18}$$

Additionally, HETP values can be calculated from mass-transfer coefficients as follows:

$$HETP = \frac{G}{K_{OG}a_e \cdot P} \cdot \frac{Ln(\lambda)}{\lambda - 1} \tag{19}$$

where λ is the absorption factor defined as m(G/L).

EXPERIMENTAL PART

Experiments were carried out in a plexiglass column of 1-in. diameter, packed with 54 inches of bales. Each bale element has the same diameter of the column and they were 18-in. long, so three elements were loaded in the column for each experiment. The aqueous solution of MEA (9.1 wt%) gets in the column through the top and is contacted counter-currently with ascending air and CO_2, which gets to the column through the bottom. The gas inlet concentration of CO_2 is 15 mol%. The absorption tests were carried out at the local atmospheric pressure (660 mm Hg) and temperature (21°C).

The bales were loaded with ion-exchange resin catalysts (Amberlyst 15) with acid sites that were previously neutralized with NaOH, since the reaction between CO_2 and MEA does not require a catalyst. Three sets of bales were prepared to evaluate the effect of superficial area (using different amounts of mesh wire cloth in each packing) and the amount of catalyst (affecting mainly void fraction). Table 1 shows the characteristics of each set of packings prepared for this work.

A total of 36 tests were performed (12 with each set of packings), varying the gas and liquid flow rates, as can be seen in Table 2.

Table 1. Physical characteristics of set of packings.

Set of packings	Superficial area of the packing, a_p (m^2/m^3)	Catalyst density (Kg/m^3)	Void fraction area of the packing, ε
Bale 1	100	64	0.803
Bale 2	200	64	0.714
Bale 3	200	128	0.630

Table 2. Experimental plan.

Test	Volumetric flow rate of gas (m^3/h) P = 1 atm. T = 25°C	F-Factor ($u_G \cdot \rho_G^{0,5}$)	Volumetric flow rate of liquid, L/h
1	0.59	0.30	4
2	1.19	0.60	
3	1.98	1.00	
4	2.77	1.40	
5	3.36	1.70	
6	3.96	2.00	
7	0.59	0.30	8
8	1.19	0.60	
9	1.98	1.00	
10	2.77	1.40	
11	3.36	1.70	
12	3.96	2.00	

Additional tests were performed to measure pressure drop to verify the flowdynamics and to have reference values to compare with the previous work of Caetano.[12] The gas flow is determined by F-factor ($u_G \cdot \rho_G^{0,5}$).

Liquid samples from the top and bottom of the column were taken when steady-state conditions were achieved. Each liquid sample was analyzed to determine total alkalinity (by titration) and CO_2 content (free CO_2 + MEA reacted CO_2). This test is performed liberating the CO_2 from the original sample using HCl, which is collected in a $Ba(OH)_2$ trap to produce a precipitate of $BaCO_3$. The amount of CO_2 in the original sample is them determine by titration of the remaining $Ba(OH)_2$ solution.[18]

With all this information, it is possible to determine the value of the product of the overall mass-transfer coefficient and the effective area ($K_{OG}a_e$). An exothermic reaction takes place when CO_2 is absorbed with MEA [see Eq. (3)]. Danckwerts[14] defines the absorption velocity of CO_2 in MEA as the summation of the gas flow that dissolves in the liquid plus the reaction rate of CO_2 with the amine, which gives the following expression:

$$N_{CO_2} \cdot a_e \cdot dz = u_L \cdot dC_{CO_2} + h \cdot \upsilon \cdot dz \tag{20}$$

On the other hand, the decrease in the MEA concentration is equal to the reaction rate of MEA with CO_2

$$-u_L \cdot dC_{MEA} = 2 \cdot h \cdot \upsilon \cdot dz \tag{21}$$

Since the amount of CO_2 dissolved in the liquid is very small in comparison with the amount reacted with the MEA,[14] this affects Eq. (20) as follows:

$$N_{CO_2} \cdot a_e \cdot dz = h \cdot v \cdot dz \tag{22}$$

substituting Eq. 21 in Eq. (22)

$$N_{CO_2} \cdot a_e \cdot dz = -\frac{u_L}{2} \cdot dC_{MEA} \tag{23}$$

On the other hand, the absorption velocity can be expressed as follows using the overall mass-transfer coefficient:

$$N_{CO_2} \cdot a_e = K_{OG} \cdot a_e \cdot \left(P_{CO_2} - P^*_{Co_2}\right) \tag{24}$$

Substituting Eq. 24, in Eq. (23)

$$-\frac{u_L}{2} dC_{MEA} = K_{OG} \cdot a_e \cdot \left(P_{CO_2} - P^*_{Co_2}\right) \cdot dz \tag{25}$$

Assuming that the mass-transfer coefficient and the effective area are constant, Eq. (25) can be integrated along the absorber as follows:

$$z = \frac{u_L}{2 \cdot K_{OG} \cdot a_e} \cdot \int_{C_{MEA_2}}^{C_{MEA_1}} \frac{1}{\left(P_{CO_2} - P^*_{CO_2}\right)} dC_{MEA} \tag{26}$$

Equation 26 was used to determine the values of $K_{OG}a_e$, since all other parameters are known for each of the 36 experiments performed in this work.

RESULTS AND DISCUSSION

The results of pressure drop obtained in this work indicated that the flowdynamic characteristics are very similar to those previously reported by Caetano,[12] as can be seen in Fig. 2. This confirms that column flow dynamics in both works are very similar.

The results of the experimental tests allowed the calculation of the overall mass-transfer coefficient ($K_{OG}a_e$) for the three sets of packings at different liquid and gas flow rates. Figure 3 shows these results as function of the gas-flow related F-factor. The three lower curves correspond to the lower liquid flow rate (4 L/h), while the upper ones correspond to higher liquid flow rates (8 L/h).

It can be seen in Fig. 3 that doubling the liquid flow produces an increase of the overall coefficient between 50 and 250%. This can be due either to an increase of the liquid-side mass transfer coefficient or to an increase of

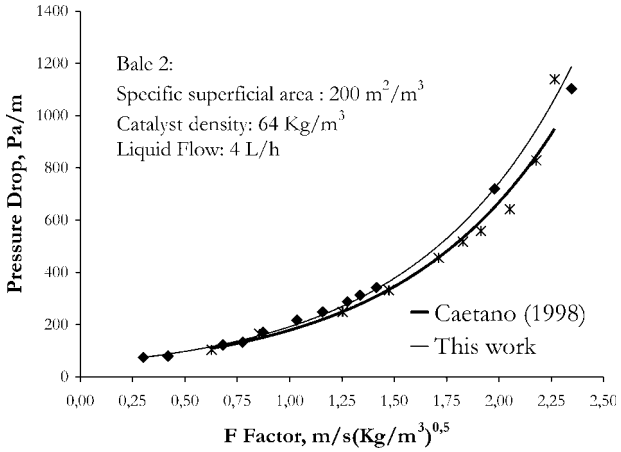

Figure 2. Effect of the gas load (F-factor) on experimental pressure drop (Bale 2).

the effective interfacial area. The increase of the liquid-phase Reynolds number increases the liquid-side mass-transfer coefficient, as has been well documented.[19] On the other hand, it is also well known that liquid hold-up in the column increases with the liquid velocity,[19] which should produce a large interfacial area for mass transfer between liquid and gas.

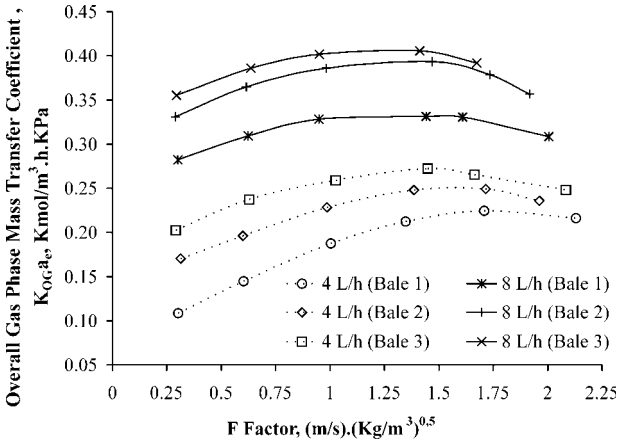

Figure 3. Effect of the gas load (F-factor) on overall gas phase mass transfer coefficient.

The trends of all the curves in Fig. 3 are very similar. In the preloading regime (approximately F-factor < 1.5), where the liquid hold-up is constant for each curve, the increase in the $K_{OG}a_e$ should be due to the increase of the gas-side mass-transfer coefficient, since in that region, the effective interfacial area and the liquid-side mass-transfer coefficient should be relatively constant. In the preloading regime, the increase of 100% in the gas velocity only increases the overall mass-transfer coefficient between 5 and 35%, indicating a moderate resistance in the gas side.

When the loading point is reached (F-factor ~ 1.5), at constant liquid flow rate, the value of $K_{OG}a_e$ levels out and then decreases as the gas velocity increases. Kister[19] argues that in the loading regime, the accumulation of liquid causes back mixing of this phase, which affects the mass-transfer efficiency due to a reduction of the driving force (concentration gradient).

The previous arguments points out that the main resistance to the mass-transfer process in this work should be in the liquid side, due to the big changes observed in the parameter $K_{OG}a_e$ when the liquid flow is doubled, in comparison to the trends observed when the gas velocity is increased. It should be also pointed out that this statement considers that the information available in previous works (Bravo and Fair[4]) shows that in the preloading region, the effective interfacial area is a weak function of the phases velocities and, consequently, the changes observed in the parameter should be essentially due to changes in the mass-transfer coefficient. Other investigators also found when absorbing CO_2 in diluted solutions of MEA that the gas phase has small resistance to the mass-transfer process.[13,14]

Figure 3 also shows the effect of the catalyst density in the mass-transfer rate between liquid and gas, when the results of bale 2 ($64\,kg/m^3$) are compared with those obtained with bale 3 ($128\,kg/m^3$) at constant superficial area ($200\,m^2/m^3$). The increase in the catalyst content by 100%, moderately increases the $K_{OG}a_e$ between 2 and 20%. Caetano[12] showed that the liquid hold-up of bale 2 is 30 to 50% lower than that of bale 3. This additional liquid in the column should generate additional area for mass transfer from the gas phase.

It can be also noticed in Fig. 3 that at constant catalyst content ($64\,kg/m^3$), the bale packing with the highest superficial area (bale 2 at $200\,m^2/m^3$) shows a $K_{OG}a_e$ value between 20 and 50% larger than the packing with the lowest superficial area (bale 1 at $100\,m^2/m^3$), at both liquid flow rates. Clearly, this is an indication of the effective mass-transfer area enhancement, when the amount of fiber-glass cloth is increased in the packing.

Although the effect of the column wall is important due to the ratio between wall surface ($160\,m^2/m^3$) and packing surface (100 to $200\,m^2/m^3$), for comparative purposes, these effects are always present for all tests.

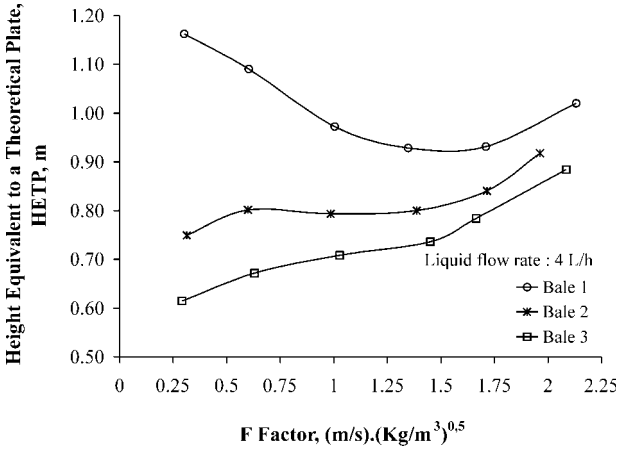

Figure 4. Effect of the gas load (F-factor) on height equivalent to a theoretical plate (4 Lt/h).

The variation of HETP as function of the F-factor are shown in Figs. 4 and 5. HETP values were calculated by substituting the experimental $K_{OG}a_e$ values into Eq. (19). First of all, it is important to notice that the HETP values range between 0.6 and 1.2 m. These values are larger than those

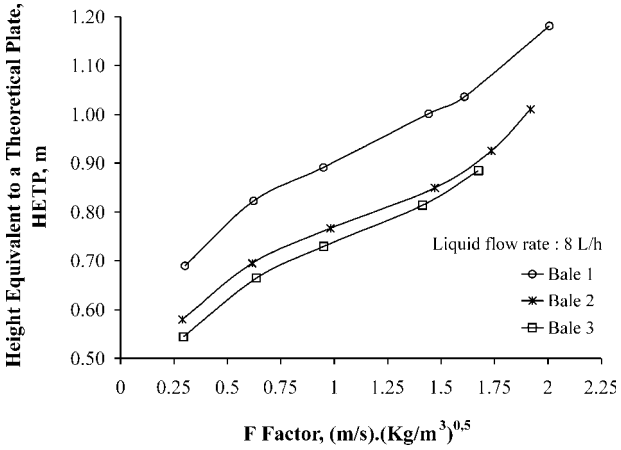

Figure 5. Effect of the gas load (F-factor) on height equivalent to a theoretical plate (8 Lt/h).

reported previously by Subawalla et al.[10] for similar bale catalytic packings in small columns, which ranged between 0.3 to 0.6 m, when distilling at total reflux organic mixtures (polar and nonpolar). This difference should be due to the difference in the nature of the chemical systems and processes employed in both works. A common trend in all curves is that HETP values increase in the loading region (F-factor > 1.5). However, before the loading point, trends are different for each packing, even though the mass-transfer coefficient increases with the F-factor.

The HETP trends for bale 1 (Fig. 4, liquid flow rate = 4 L/h) differ from those for bales 2 and 3, eventhough the $K_{OG}a_e$ trends for all bales are similar. The HETP values are directly proportional to gas flow rate and inversely proportional to $K_{OG}a_e$ values. The main cause for the strange trends in bale 1 is that at low liquid and gas flow rates, the percentage change in $K_{OG}a_e$ with gas flow rate is greater than the percentage change in the gas flow rate itself. Therefore, HETP initially decreases and then increases as the increase in gas flow rate more than compensates for the increase in mass transfer. This behavior is not observed in bales 2 and 3, possibly because they posses a greater specific surface area and lower void fraction.

Figures 6 and 7 show parity plots to assess the validity of the models of Subawalla et al.[10] and Bravo and Fair.[4] The predictions made with the model of Zhen and Xu[17] were completely different for all the points (predictions were 500% larger than the experimental values). It can be noticed

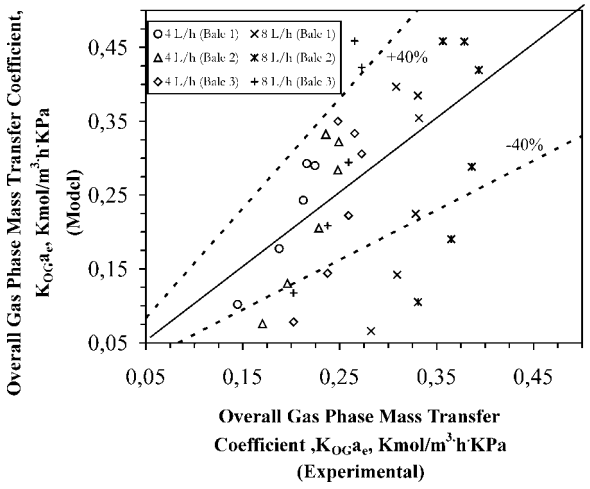

Figure 6. Comparison of $K_{OG}a_e$ predicted by Subawalla et al.[10] correlation.

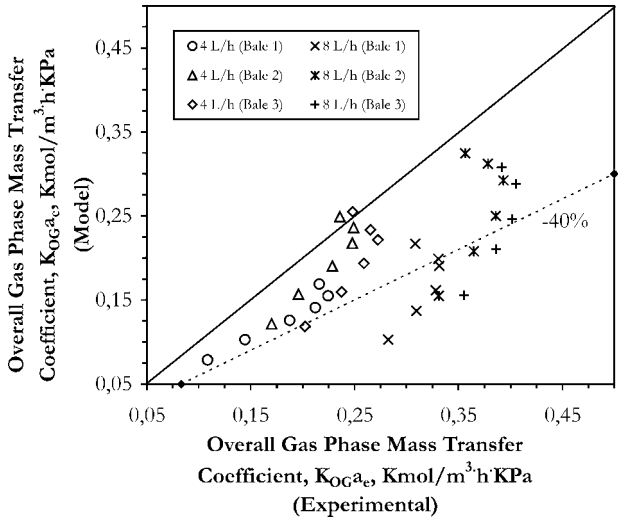

Figure 7. Comparison of $K_{OG}a_e$ predicted by Bravo and Fair[5] correlation.

that most of the deviations of the Subawalla model fall within $\pm 40\%$. Larger deviations are noticed at very low gas velocities, where the model tends to under predict the mass-transfer coefficient.

The predictions made with the model of Bravo and Fair are in 95% of the cases lower than the experimental values, as can be seen in Fig. 6, but most of the points fall within the -40% bound. These results shown that there is still a need to significantly improve the available models to get a good and accurate prediction of the mass transfer behavior of bale-type catalytic packing.

CONCLUSIONS

The mass transfer characteristics of the bale-type catalytic packing were evaluated in a 1-in. column, absorbing CO_2 in a diluted solution of MEA. The following conclusions can be drawn from this work:

- The main mass transfer resistance in the absorption tests performed in this work is in the liquid phase, although the resistance of the gas side cannot be completely neglected.
- The mass-transfer efficiency of the bale-type packing can be adjusted with the amount of fiberglass cloth used in the manufacture of

the bales. When the amount of cloth per volume of column is doubled, the product of the mass-transfer coefficient and the effective area increases 20 to 50%.

- The amount of catalyst placed inside the pockets of the bales, which should depend on the specific reaction requirements for each application, affects the flowdynamic behavior of the column, since the void fraction depends mainly on this parameter. The increase of the catalyst density in the column increases the liquid hold-up, which improves the effective mass-transfer area.
- There is a need to develop more accurate mass transfer models for the bale-type catalytic packing.

NOMENCLATURE

a_e	Specific interfacial mass-transfer area per volume of column, L^2/L^3
a_g	Drops superficial area per unit volume, L^2/L^3
a_p	Packing superficial area per unit volume, L^2/L^3
a_w	Column wall area per unit volume, L^2/L^3
a_{wetp}	Packing wet area per unit volume, L^2/L^3
a_{wetw}	Wall wet area per unit volume, L^2/L^3
C_{RNH2}	Solvent (RNH_2) concentration, mole/L^3
C_{Ai}	Concentration of solvent A at the interface, mole/L^3
C_{CO_2}	CO_2 concentration, mole/L^3
Ca_L	Liquid capillarity number, dimensionless
C_{MEA}	MEA concentration in the liquid, mole/L^3
C_{STE}	Solvent concentration, mole/L^3
D_{CO_2}	Liquid diffusivity of component A, L^2/θ
D_G	Gas diffusion coefficient of solute, L^2/θ
D_L	Liquid diffusion coefficient of solute, L^2/θ
d_p	Nominal diameter of the packing element, L
D_{STE}	Solvent diffusivity in the liquid solution, L^2/θ
E	Enhancement factor (ratio k_L/k_L^0), dimensionless
E_i	Enhancement factor (ratio k_L/k_L^0) when $N_{Ha} \rightarrow \infty$, dimensionless
F	F-Factor, $[L/\theta\ (M/L^3)^{0.5}]$
Fr_L	Liquid Froude number, dimensionless
g	gravity acceleration, L/θ^2
G	Gas superficial molar velocity per unit volume, mole/$\theta \cdot L^2$

h	Liquid hold-up, L^3/L^3
H	Packing bed height, L
HETP	Height equivalent to a theoretical plate, L
k_2	Second-order reaction rate constant, $L^3/\theta\cdot$mole
k_G	Gas-side mass-transfer coefficient, mole/$L^2\cdot\theta\cdot(F/L^2)$
k_L	Liquid-side mass-transfer coefficient, mole/$L^2\cdot\theta\cdot(F/L^2)$
k_L^0	Liquid-side mass-transfer coefficient for purely physical absorption, mole/$L^2\cdot\theta\cdot(F/L^2)$
K_{OG}	Overall volumetric mass-transfer coefficient referred to the gas side, mole/$L^2\cdot\theta\cdot(F/L^2)$
K_{OGg}	Overall volumetric mass-transfer coefficient referred to the gas side for drops, mole/$L^2\cdot\theta\cdot(F/L^2)$
K_{OGp}	Overall volumetric mass-transfer coefficient referred to the gas side for the packing, mole/$L^2\cdot\theta\cdot(F/L^2)$
K_{OGw}	Overall volumetric mass-transfer coefficient referred to the gas side for the wall, mole/$L^2\cdot\theta\cdot(F/L^2)$
L	Liquid molar superficial velocity, mole/$\theta\cdot L^2$
m	Slope of the equilibrium curve, gas mole fraction/liquid mole fraction
M	Dimensionless parameter defined by Eq. 7
N_A	Mass transfer rate of solute per unit of interfacial area, mole/$\theta\cdot L^2$
N_{Ha}	Hatta number, dimensionless
P	Pressure, F/L^2
P_A	Partial pressure of component A, F/L^2
P_{CO_2}	CO_2 partial pressure, F/L^2
$P^*_{CO_2}$	CO_2 partial pressure in equilibrium with liquid, F/L^2
P_{Ai}	Component A partial pressure at the interface, F/L^2
Re_G	Reynolds number for the gas, dimensionless
Re_L	Reynolds number for the liquid, dimensionless
Sc_G	Schmidt number for the gas, dimensionless
Sc_L	Schmidt number for the liquid, dimensionless
Sh_G	Sherwood number for the gas, dimensionless
Sh_G	Sherwood number for the liquid, dimensionless
T	Temperature, °K
U_L	Liquid superficial velocity, L/θ
We_L	Weber number for liquid, dimensionless
x_A	Mole fraction of component A in the liquid, dimensionless
x_{Ai}	Mole fraction of component A of the liquid in the interface, dimensionless
z	Coordinate axis (mass transfer direction)

Greek Letters

λ	Absorption factor, dimensionless
$\Delta P/Z$	Pressure drop per unit length, F/L^3
σ_L	Liquid superficial tension, F/L
σ_C	Critical superficial tension, F/L
ρ_G	Gas density, M/L^3
ρ_L	Liquid density, M/L^3
υ	Reaction rate, $mol/L^3 \cdot \theta$
μ_L	Liquid viscosity, $M/L \cdot \theta$

ACKNOWLEDGMENTS

Authors want to express their gratitude to Dr. Manuel Pacheco, who provided significant support in the design, calculations, and interpretation of the absorption tests. Also, the laboratory help of Mr. Raúl Navarro and Mrs. Douglaines Marcano is acknowledged.

REFERENCES

1. Castillo, C.; Escalante, L.; González, J.C. Destilación Catalítica: Aplicaciones de una tecnología emergente. Visión Tecnol. **1993**, *1* (2), 13–21.
2. Onda, K.; Sada, E.; Takeuchi, H. Gas absorption with chemical reaction in packed columns. J. Chem. Eng. Jpn **1968**, *1*, 62–68.
3. Onda, K.; Takeuchi, H.; Okumoto, Y. Mass transfer coefficients between gas and liquid phases in packed columns. J. Chem. Eng. Jpn **1968**, *1*, 56–62.
4. Bolles, W.; Fair, J.R. Improved mass transfer model enhance packed-column design. Chem. Eng. **1982**, *89* (14), 109.
5. Bravo, J.L.; Fair, J.R. Generalized correlation for mass transfer on packed distillation columns. Ind. Eng. Chem. Proc. Des. Dev. **1982**, *21*, 162–170.
6. Wagner, I.; Stichlmair, J.; Fair, J.R. Mass transfer in beds of modern, high-efficiency random packings. Ind. Eng. Chem. Res. **1997**, *36*, 227–237.
7. Pinjala, V.; DeGarmo, J.L.; Ulowetz, M.A.; Marker, T.; Luebke, C. Rate-based modeling of reactive distillation systems. AIChE Anual Meeting, Miami Beach, FL, 1992.

8. Zheng, Y.; Xu, X. Study on catalytic distillation processes. Part II: simulation of catalytic distillation processes—quasi-homogeneous and rate-based model. Trans. Inst. Chem. Eng. **1992**, *70* (Part A), 465.
9. Sundmacher, K.; Hoffmann, U. Development of a new catalytic distillation process for fuel ethers via a detailed nonequilibrium model. Chem. Eng. Sci. **1996**, *51* (10), 2359–2368.
10. Subawalla, H.; González, J.C.; Seibert, F.; Fair, J.R. Capacity and efficiency of reactive distillation bale packing: modeling and experimental validation. Ind. Eng. Chem. Res. **1997**, *36*, 3821–3832.
11. Aroonwilas, A.; Adisorn, J.; Veawab, A.; Tontiwachwuthikul, P. Behavior of the mass transfer coefficient of structured packings in CO_2 absorbers with chemical reactors. Ind. Eng. Chem. Res. **1999**, *38*, 2044–2050.
12. Caetano, M.G. Evaluación de las características de la hidrodinámica en empaques de destilación catalítica tipo bale. Trabajo Especial de Grado. UCV, Ingeniería química, 1998.
13. Weiland, R. Reaction kinetics of CO_2 with MEA, DEA, and MDEA and in MDEA-based blends. Research Report, RR-151; Gas Processors Association: Texas, 1996.
14. Danckwerts, P.V. *Gas Liquid Reaction*; McGraw Hill: New York, 1970.
15. Arai, R. Application of catalitic distillation in the refining and the chemical industries. National Petroleum Refiners Association—Annual Meeting, Los Angeles, 1986.
16. Smith, L.A. Catalytic Distillation Process. U. S. Pattent 4,307,254, 1983.
17. Zheng, Y.; Xu, X. Study on catalytic distillation processes. Part I: mass transfer characteristics in catalyst bed whit in the column. Trans. I. Chem. E **1992**, *70*, 459.
18. PDVSA. Intevep S.A. Informe técnico INT-00791,83.
19. Kister, H. *Distillation Design*; McGraw Hill: USA, 1992.

Received August 2002
Revised February 2003